J. Fluid Mech. (1971), *vol.* 49, *part* 2, *pp.* 279–288
Printed in Great Britain

On sideways diffusive instability

By J. E. HART

Department of Applied Mathematics and Theoretical Physics,
University of Cambridge

(Received 22 January 1971)

We consider the stability of the motion generated in a differentially heated vertical slot filled with a linearly stratified salt solution. The theoretical mean motion field between infinite plates is a function of the Rayleigh number $R_s = g\beta(\partial S_0/\partial z)D^4/k_s\nu$. If R_s is zero the salinity does not enter the problem and one finds instability in the form of stationary rolls which obtain most of their energy from the basic velocity field. Even at very small R_s of order -1000 these shear instabilities are replaced by diffusively destabilized convective rolls which appear at a thermal Rayleigh number $R_a = g\alpha\Delta TD^3/k_T\nu$ which is two orders of magnitude less than that required for the shear generated modes. The present calculations, which take proper account of both the mean fields and the boundary conditions, give results which compare somewhat more favourably with the experimental results of Thorpe, Hutt & Soulsby (1969) than the theory put forward by these authors. It is shown why their theory, which deals with different boundary conditions from those in the experiment, gives adequate results as R_s tends to negative infinity.

1. Introduction

There has been considerable interest lately, especially amongst geophysical fluid dynamicists, in flows which can become convectively unstable as a result of differential diffusion. This occurs when the generally stabilizing effect of one component is reduced by diffusion allowing a release of potential energy of an unstable component. Thermohaline convection in the presence of vertical temperature and salinity gradients between horizontal plates is a well-known example of this phenomena (for examples see Stern 1960, or Baines & Gill 1969). In this type of convective instability the cells are rectangular† and the motion results from diffusion away from vertically displaced parcels. Blumsack (1967) and Thorpe, Hutt & Soulsby (1969), hereafter THS, considered a different type of instability which occurs in the presence of both vertical and horizontal gradients of heat and salt. In these situations the cells are tilted and the motion results from diffusion away from parcels displaced sideways, or perhaps more correctly, along sloping surfaces. Both Blumsack and THS give simple physical explanations of the instability. This instability is not restricted to situations in which both diffusive components affect the density, nor do the components

† This is to say that the theoretical eigenfunction can be written as $f(z, t)\, e^{ikx}$ where f is real.

need to be heat and salt, so long as the two diffusivities are unequal. McIntyre (1970) has shown how angular momentum and temperature can act as the agents to diffusively destabilize a circular baroclinic vortex.

There is some experimental evidence for this type of sideways diffusive instability. THS observe the onset and subsequent development of rolls in a vertical channel, heated from the sides, containing a linearly stratified salt solution. D. J. Baker (private communication) has observed layers in a rotating stratified fluid which may be due to McIntyre's related mechanism. However, there has been no theory put forward which satisfies all the experimental constraints. This paper presents an attempt to construct such a theory for the thermohaline case. The linearized stability problem is formulated in §2. Section 3 contains an asymptotic solution which shows the relation between this work and the theory of THS. The numerical calculation of the complete neutral stability curve is outlined in §4 and the results are compared with the available experimental data in §5.

2. Formulation

We consider the experimental setup in figure 1. The fluid is initially linearly stratified and the superimposed velocity–temperature–salinity fields are set up by imposing a quasi-statically increasing temperature difference across the plates at $x^* = \pm\frac{1}{2}D$. These are assumed to be rigid, perfectly conducting to heat, and perfectly insulating to salt. The wall at $z^* = -\frac{1}{2}L$ is a rigid insulator, that at $\frac{1}{2}L$ a free insulator. We suppose that L/D is sufficiently large that for measurements conducted near the centre of the apparatus the assumption of a steady parallel mean flow with $\partial S_0/\partial z$ equal to its initial value will be valid. This assumption will be clarified later. Within the Boussinesq approximation the full non-dimensional equations are

$$\frac{R_a}{P_r}\frac{d\mathbf{u}}{dt} = -\nabla p + \nabla^2\mathbf{u} + (T-S)\,\hat{z}, \quad \nabla\cdot\mathbf{u} = 0, \tag{2.1}$$

$$R_a\, dT/dt = \nabla^2 T, \tag{2.2}$$

$$HR_a\, dS/dt + R_s w = \nabla^2 S. \tag{2.3}$$

The non-dimensional parameters are the thermal Rayleigh number

$$R_a = g\alpha\Delta T D^3/\kappa_T \nu$$

the salinity Rayleigh number $R_s = g\beta(\partial S_0/\partial z)\,D^4/\kappa_s\nu$, the Prandtl number $P_r = \kappa_T/\nu$ and the Schmidt number $H = \kappa_T/\kappa_s$. Velocities have been scaled by $g\alpha\Delta T D^2/\nu$, lengths by D, temperature by ΔT, and salinity by $\alpha\Delta T/\beta$. In the above definitions g is the gravitational acceleration, α the coefficient of thermal expansion, β the coefficient of volumetric expansion, κ_T the diffusitivity of temperature, κ_s the diffusivity of salt, and ν the kinematic viscosity.

With the infinite channel assumption we must satisfy boundary conditions

$$T = \pm\tfrac{1}{2}, \tag{2.4}$$

$$S_x = 0, \tag{2.5}$$

and

$$v = w = u = 0 \quad \text{at} \quad x = \pm\tfrac{1}{2}. \tag{2.6}$$

The steady parallel flow equations are exactly linear:

$$w_{oxx}+T_0-S_0 = 0, \tag{2.7}$$

$$T_{oxx} = 0, \tag{2.8}$$

$$S_{oxx}-R_s w_0 = 0. \tag{2.9}$$

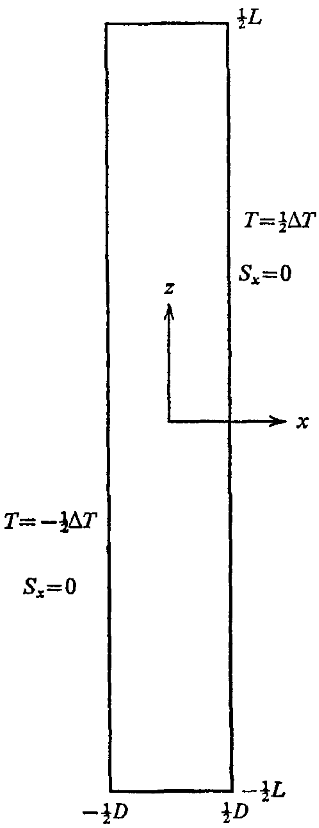

FIGURE 1. Geometry for the problem. The box initially contains a linearly stratified salt solution.

The solution of these equations is

$$T_0 = x, \tag{2.10}$$

$$S_0 = x-[\cosh Mx \cos Mx(1+A)+\sinh Mx \sin Mx(A-1)]/B, \tag{2.11}$$

and
$$W_0 = [\cosh Mx \sin Mx - A \sinh Mx \cos Mx]/2M^3B, \tag{2.12}$$

where
$$A = \tan \tfrac{1}{2}M/\tanh \tfrac{1}{2}M,$$

and
$$B = \sin \tfrac{1}{2}M/\sinh \tfrac{1}{2}M + \cosh \tfrac{1}{2}M/\cos \tfrac{1}{2}M.$$

Thus the solution depends on the single parameter

$$M = (-\tfrac{1}{4}R_s)^{\frac{1}{4}}. \tag{2.13}$$

Figure 2 shows how the profiles change as M increases. There is always a motion field although this becomes small as M becomes large. The non-dimensional horizontal density gradient (given by $S_{0x}-1$) is also a function of M, and becomes zero except in narrow wall regions of width M^{-1} as M becomes large. These changes reflect the stabilizing effect of the vertical salinity gradient.

To examine the stability of (2.10)–(2.11) we write perturbed variables proportional to $\exp[ikz+\omega t]$ and linearize equations (2.1)–(2.3). We thus assume

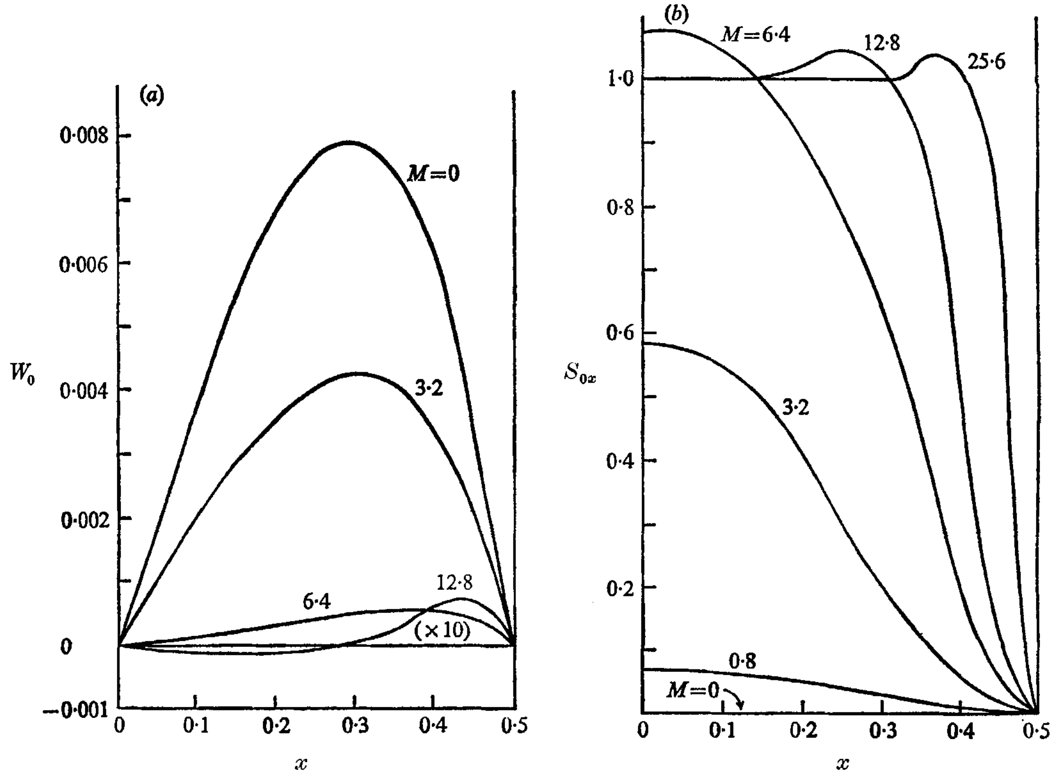

FIGURE 2. The basic fields as a function of $M=(-\frac{1}{4}R_s)^{\frac{1}{4}}$. (a) The velocity, antisymmetric about $x=0$, and (b) the horizontal salinity gradient, symmetric about $x=0$.

two-dimensional transverse rolls.† With $d\equiv d/dx$, $w=\psi_x$, and $u=-\psi_z$, the perturbation equations are:

$$-\frac{R_a\omega}{P_r}(d^2-k^2)\psi+(d^2-k^2)^2\psi-ik\frac{R_a}{P_r}[W_0(d^2-k^2)\psi-\psi d^2W_0]+dT-dS=0, \tag{2.14}$$

$$-R_a\omega T+(d^2-k^2)T+ikR_a\psi-ikR_aW_0T=0, \tag{2.15}$$

$$-HR_a\omega S+(d^2-k^2)S+ikHR_a dS_0\psi-ikHR_aW_0S-R_s d\psi=0, \tag{2.16}$$

which must be solved subject to

$$\psi=d\psi=T=dS=0 \quad \text{at} \quad x=\pm\tfrac{1}{2}. \tag{2.17}$$

† Under certain conditions these can be shown to be the most unstable (THS, appendix B) but for the general mean fields considered here a Squires theorem cannot be proved.

3. Asymptotic solution for large $-R_s$

The solution presented by THS is a solution of (2.14)–(2.16) in which

$$\omega = 0,\ W_0 \equiv 0,\ S_{0x} \equiv 1,$$

and only the boundary condition on ψ is satisfied. The prediction of their model gave results for large $-R_s$ which were quite consistent with experiment. In this section we show that the leading order asymptotic solution of the full problem for large $-R_s$ gives their result and confirms their hypothesis about the effect of mean flow and boundary conditions in this limit.

We consider the solution for $\omega = 0$, $R_s \to -\infty$, $H \gtrsim O(1)$, and $P_r \gtrsim O(1)$. In this limit $W_0 \doteq 0$ and $S_{0x} \doteq 1$ except in boundary layers of thickness $-R_s^{-\frac{1}{4}}$. Thus we expect the solution to contain both interior and boundary components, but as yet we do not know what scales to use for the critical values R_a and k. We assume the consistent solution will have $kR_aH \sim -R_s$ and $k \gg 1$, assumptions which are justified *a posteriori*. Essentially by trial and error one can find that the proper expansion parameter is $-R_s^{-\frac{1}{6}}$. However, rather than proceed with a formal analysis we take a more heuristic approach to obtain the leading order solution. Near the walls normal derivatives will dominate tangential derivatives ($\sim k$) and boundary-layer equations can be written as

$$d^4\psi + dT - dS = ikR_aP_r^{-1}[W_0d^2\psi - \psi d^2W_0] + O(d^2k^2\psi), \tag{3.1}$$

$$d^2T + ikR_a\psi = ikW_0R_aT + O(k^2T), \tag{3.2}$$

and

$$d^2S - R_sd\psi = -ikHR_adS_0\psi + ikHR_aW_0S + O(k^2S). \tag{3.3}$$

Note $dS_0 \lesssim 1$ and $W_0 \lesssim O(-R_s^{-\frac{1}{2}})$ so that the general boundary-layer solution of (3.1)–(3.3) is

$$\psi_b = \sum_{i=1}^{4} a_i e^{r_ix} + O(a_ik^2/|R_s|^{\frac{1}{2}}), \tag{3.4}$$

where the a_i are constants and the r_i are the four roots $(\frac{1}{4}R_s)^{\frac{1}{4}}$. Since we are considering only the physically realistic case with $R_s \leqslant 0$ boundary-layer solutions exist. The thickness of these layers is the same as those in the basic flow.

In the interior the equations become

$$k^4\psi + dT - dS = O(d^2k^2\psi), \tag{3.5}$$

$$(d^2-k^2)T + ikR_a\psi = 0, \tag{3.6}$$

and

$$(d^2-k^2)S + ikHR_a\psi - R_sd\psi = 0. \tag{3.7}$$

The solutions are

$$\psi_i = a_5e^{r_5x} + a_6e^{r_6x} + O(a_5r_5^2/k^2), \tag{3.8}$$

$$T_i = (iR_a/k)(a_5e^{r_5x} + a_6e^{r_6x}) + a_7e^{kx} + a_8e^{-kx}, \tag{3.9}$$

and

$$S_i = k^{-2}(ikHR_a - R_sd)(a_5e^{r_5x} + a_6e^{r_6x}) + a_7e^{kx} + a_8e^{-kx}, \tag{3.10}$$

where

$$r_{5,6} = -\frac{ikR_a(H-1)}{2R_s} \pm \frac{1}{2R_s}(-k^2R_a^2(H-1)^2 - 4R_sk^6)^{\frac{1}{2}}. \tag{3.11}$$

The eigenvalue equation is obtained by applying the eight boundary conditions (2.17). The resulting set of linear algebraic equations can be satisfied to order

M/k^{-1} provided the condition $\psi = 0$ at $x = \pm\frac{1}{2}$ is satisfied exactly by the interior solution. This is a reflection of the ability of the wall layers to dominate the differentiated boundary conditions $d\psi = dS = 0$. Using (3.8) and (3.11) this gives

$$R_a^2(H-1)^2 = \frac{4n^2\pi^2R_s^2}{k^2} - 4k^4R_s, \tag{3.12}$$

where n must be an integer.

The most unstable mode occurs for $n = 1$ and

$$k = 1{\cdot}30(-R_s)^{\frac{1}{6}}, \tag{3.13}$$

whence

$$R_a(H-1) = 5{\cdot}90(-R_s)^{\frac{5}{6}}. \tag{3.14}$$

The error factor for the above expressions is $O(R_s^{-\frac{1}{18}})$. Conditions (3.13) and (3.14) are exactly those obtained by THS,† although their higher-order eigenvalue corrections and the eigenfunctions will not agree with the results of this analysis. Since the rolls are much wider than they are tall the effects of the walls and of the non-zero velocity and horizontal density gradient fields enter as a higher-order correction to the basic interior balance between vertical diffusion and advection. Thus one can see why the 'free-boundary' solution of THS which retains the correct interior balance seems to work.

It is relatively straightforward to include non-zero ω in the above calculation, although the final eigenvalue equation corresponding to (3.12) has to be solved numerically. One finds that the instability *is* monotonic ($\omega_i = 0$) and that dimensional e-folding times (under the experimental conditions of THS) on the order of 5 min are obtained at Rayleigh numbers 5% supercritical, increasing as $-R_s$ increases.

The above asymptotic theory predicts transition points in reasonable agreement with the experimental data provided $-R_s > 3\times10^6$. Below this value one expects the boundaries and mean flow to play an important part in determining the neutral curve. The next sections describe the numerical solution of the complete stability problem.

4. Numerical calculations

Equations (2.14)–(2.17) are solved numerically using the Galerkin method (Mikhlin 1964). We expand ψ, T and S in complete sets of functions satisfying the boundary conditions (2.17). We write

$$\psi = \sum_{i=1}^{N} a_iY_i, \tag{4.1}$$

$$T = \sum_{i=1}^{N} b_iQ_i, \tag{4.2}$$

$$S = \sum_{i=1}^{N} c_i dQ_i/\lambda_i. \tag{4.3}$$

† Note that their parameters are defined differently from ours. In the present context the correspondence is that their $R_x = R_a(H-1)/\pi^4$ and $R_z = R_s/\pi^4$.

The co-ordinate functions are given by orthogonal solutions of

$$d^2Q_i + \lambda_i^2 Q_i = 0$$

and
$$d^4Y_i - \mu_i^4 Y_i = 0,$$

with real eigenvalues λ_i and μ_i. The expansions are substituted into (2.14)–(2.17). The resulting equations are operated on by

$$\int_{-\frac{1}{2}}^{\frac{1}{2}} Y_j dx, \quad \int_{-\frac{1}{2}}^{\frac{1}{2}} Q_j dx, \quad \text{and} \quad \int_{-\frac{1}{2}}^{\frac{1}{2}} dQ_j dx,$$

respectively, thus converting the original set of differential equations into a matrix eigenvalue problem. By using suitable transformations based on the odd

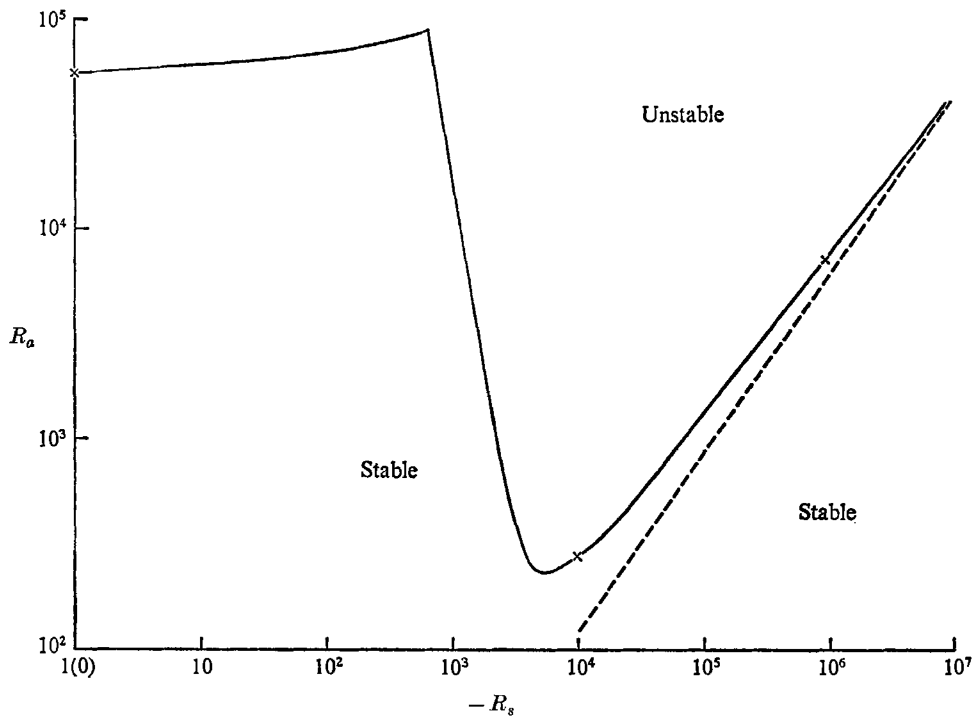

FIGURE 3. Critical (neutral) curve for $P_r = 6{\cdot}7$, $H = 101$. The crosses indicate points where the complete eigenvalue problem was solved (see text) and the dashed line represents the asymptotic result (3.14).

symmetry of the basic flow (Hart 1970) one can derive an eigenvalue problem for ω with real elements. Solving this numerically we have verified that for $H = 101$ (salt and heat) and $P_r = 6{\cdot}7$ (water) overstability does not occur and hence one can evaluate the details of the neutral curves by setting $\omega = 0$ and finding the zeros of the residual determinant. The value of N needed for convergence depends on R_s. For $R_s \sim 0$ one needs $N \geqslant 10$, for $-10^5 < R_s < -10^3$ $N \geqslant 6$, and for $R_s < -10^5$, $N > 6$, increasing as $-R_s$ becomes larger (presumably to resolve the $-R_s^{-\frac{1}{4}}$ boundary layers). For $-R_s > 10^7$ one can safely use the asymptotic result of §3. This is preferable since the final matrix is $3N \times 3N$.

Figures 3 and 4 show the numerical results. The crosses indicate points at which the complete matrix eigenvalue problem was solved for ω. The solid lines are constructed from some thirty points. In the crossed cases $\omega_i \sim 0$ to within the accuracy of the subroutine used to find it. There is a marked transition between two régimes. From previous work (Birikh *et al.* 1968, Hart 1971) we know that the instability at $R_s = 0$ is a shear instability, the perturbations obtaining most

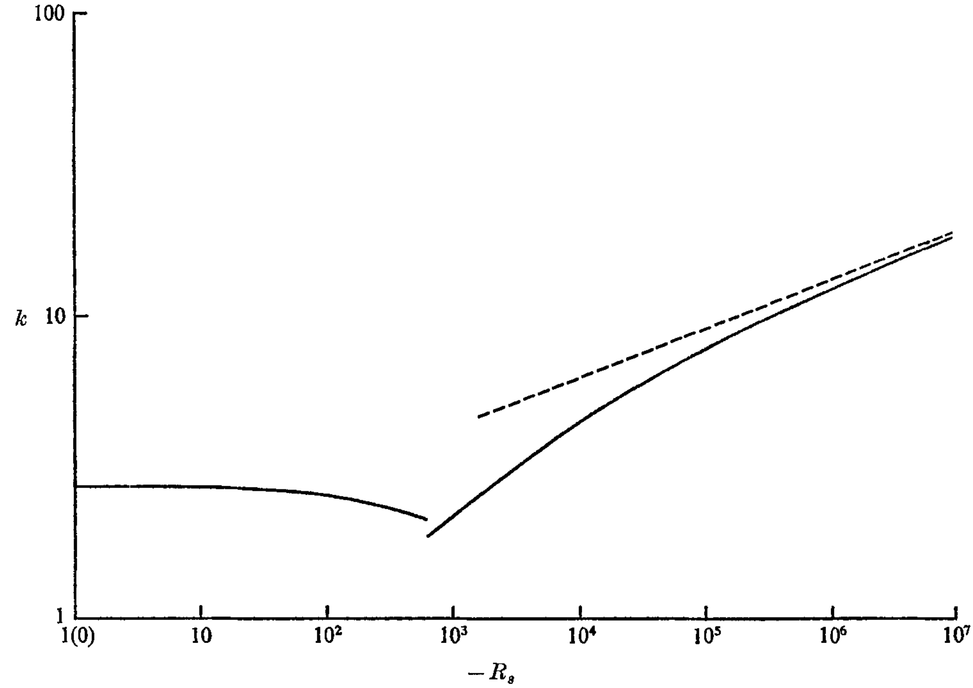

FIGURE 4. Wave-numbers for neutral stability. $P_r = 6{\cdot}7$, $H = 101$.
The dashed line represents the asymptotic result (3.13).

of their energy from the basic velocity field at the centre of the slot. The structure of the neutral curve suggests that the flow is unstable to this type of instability until $R_s \sim -1000$ where the sideways diffusive mechanism takes over. It is interesting that this double diffusive mechanism is so strong. The sideways temperature difference needed to destabilize a weak vertical salinity gradient is very small indeed (with water and a 1 cm gap $R_a = 250$ is attained with $\Delta T = 0{\cdot}017\,°\mathrm{C}$). This very low value partially explains why it has proved difficult to maintain a vertical salinity gradient in the laboratory without 'accidentally' forming layers, although many laboratory situations correspond to the more difficult $L/D \sim 1$ (time-dependent) stability problem. At these intermediate R_s the interior horizontal salinity gradient is sufficiently non-zero to destabilize the flow. It is not yet equal to 1 for all x, and this fact, coupled with the damping at the walls, yields a neutral curve above that of the previous section. As $-R_s$ increases the damping effect of the stable vertical stratification increases so that k and R_a become larger, ultimately going as $-R_s^{\frac{1}{6}}$ and $-R_s^{\frac{5}{6}}$ respectively.

5. Comparison with experiment and conclusions

Figure 5 shows the detailed comparison between the theory and the measurements taken from figures 9 and 10 of THS. There is an error in the published scale of the abscissa of figure 9, confirmed by S. Thorpe (private communication), which should give $-R_x$ ten times the values indicated. We see that the complete theory gives more favourable agreement with the data than does the approximate

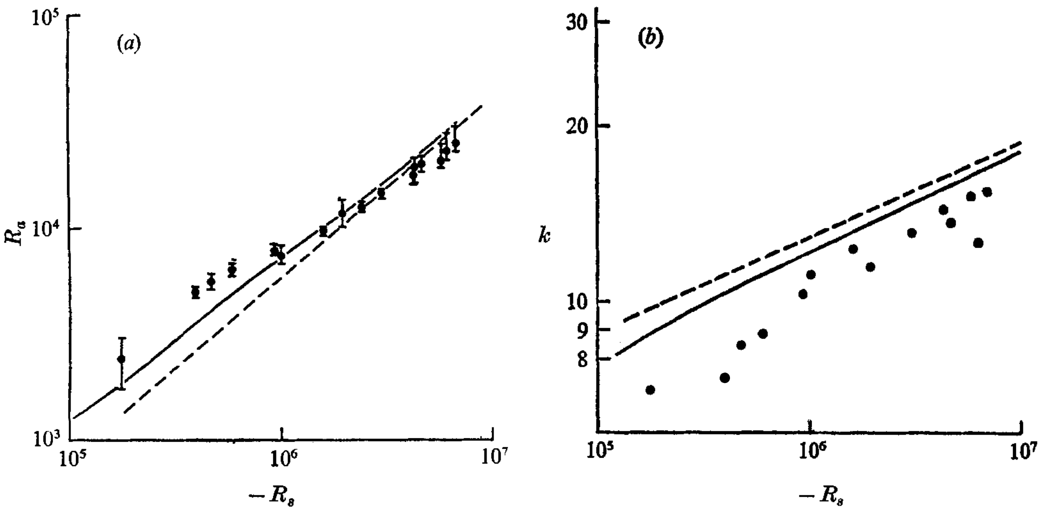

FIGURE 5. Comparison with the experimental results of THS. Solid lines represent the complete (numerical) theory, dashed lines the asymptotic results.

theory, especially for lower $-R_s$ where the latter is less valid. Note that the 'first-order correction' of THS predicts a similar behaviour but this is regarded as fortuitous since as seen in § 3 corrections to the leading order asymptotic theory must involve the boundary conditions which they have treated incorrectly. There is still a significant discrepancy but this may well be due to the difficulty in observing the onset of infinitesimal disturbances, a fact which was reflected in the cell structure which did not appear to have the symmetric form e^{ikz} required by linear theory. Theoretically the neutral curves $R_a(k)$ at large $-R_s$ tend to have $|\partial^2 R_a/\partial k^2| \ll 1$ where $\partial R_a/\partial k = 0$, so that at slightly supercritical conditions a wide band of wave-numbers can be excited.

For $-R_s > 6\times 10^6$ the points seem to be lower than the theoretical limit. If this is significant it suggests we look at the validity of the basic flow model. Aside from the parallel flow assumption, the other assumptions made in deriving (2.10)–(2.12) were: (i) T_0 (also W_0 and S_0) are independent of time; (ii) $S_{0z}(x,z,t) = S_{0z}(x,0,0)$; (iii) $T_{0z} = 0$ away from the end regions $z = \pm L/2D$. In the absence of quantititative basic flow measurements or a complete theory we can only speculate as to the validity of these assumptions. Since the mean flow will tend to mix up the initial salinity gradient (ii) puts an upper limit on the time one can run an experiment, and hence the quasi-static assumption (i) can never be satisfied exactly. This limit, estimated as the time for particle advection from one end to the centre of the box is

$$\tau \sim L/|W_0|_{\max} \cdot g\alpha\Delta T_{\mathrm{crit}} D^2/\nu,$$

which is of order 10 h for $-R_s > 10^6$. We expect both assumptions (i) and (ii) will be valid for experiments run on this time scale. In the case of (iii) we expect that T_{0z}, if non-zero, would be positive and hence would raise the effective $-R_s$ and increase the discrepancy between theory and experiment. Another possibility is the non-Boussinesq behaviour of the fluid at the high temperature differences ($\sim$ 10° C) needed in these experimental cases.

In summary, we have shown that the complete stability theory for the flow in a differentially heated vertical channel filled with a linearly stratified salt solution yields critical Rayleigh and wave-numbers which are in somewhat better agreement with the available data than the predictions of the previous theories, which do not deal with the mean flow or boundary conditions applicable to the experiment. The present results support the interpretation that the observed motions arise from diffusive destabilization.

This research was carried out while the author was visiting the Department of Applied Mathematics and Theoretical Physics, Cambridge University, on a N.A.T.O. fellowship. The author would like to thank Dr S. A. Thorpe for his interest and helpful comments on this problem.

REFERENCES

Baines, P. G. & Gill, A. E. 1969 *J. Fluid Mech.* **37**, 289–306.

Birikh, R. V., Gershuni, G. Z., Zhukovitskii, E. M. & Rudakov, R. N. 1968 *Prikl. Mat. i. Mekh.* **32**, 256–263.

Blumsack, S. L. 1967 *Geophys. Fluid Dynamics Summer Notes* II, 1–17. Woods Hole Oceanographic Institution.

Hart, J. E. 1970 Ph.D. Thesis, Massachusetts Institute of Technology.

Hart, J. E. 1971 *J. Fluid Mech.* (in the press).

McIntyre, M. E. 1970 *Geophys. Fluid Dynamics*, **1**, 19–57.

Mikhlin, S. G. 1964 *Variational Methods in Mathematical Physics*. Pergamon.

Stern, M. 1960 *Tellus*, **12**, 172–175.

Thorpe, S. A., Hutt, P. K. & Soulsby, R. 1969 *J. Fluid Mech.* **38**, 375–400.